

## MULTI-CLASS OPTICAL-CDMA NETWORK USING OPTICAL POWER CONTROL

**N. Tarhuni**

Communications Engineering Lab.  
Helsinki University of Technology  
Otakaari 5A 02150 Espoo, Finland

**M. Elmusrati**

Control Engineering Lab.  
Helsinki University of Technology  
Otaniementie 17 02150 ESPOO, Finland

**T. Korhonen**

Communications Engineering Lab.  
Helsinki University of Technology  
Otakaari 5A 02150 Espoo, Finland

**Abstract**—In this paper we use optical power control to support multirate transmission over temporal optical CDMA networks. We apply the centralized power control algorithm to set the transmit power of the users' optical sources in order to satisfy a given target QoS. In addition, optical amplifiers are included to enhance the overall system performance while the Amplified Spontaneous Emission (ASE) is considered as the main noise source. The objective function defined as the sum of the transmitted optical power from all nodes is minimized subject to a signal-to-interference (SIR) constraint. Moreover, the network feasibility, defined as the ability to evaluate a power vector that satisfy the target SIR, is discussed in terms of the spectral radius of the network interference matrix. Next, the spectral radius of the network interference matrix is investigated and modeled as a truncated Gaussian distribution. Last, a rate reduction algorithm, categorized in terms of the number of nodes involved in the process of rate reduction, is proposed to increase the network feasibility. As more nodes are added to the rate reduction campaign, the network feasibility is significantly enhanced. For typical network parameters we find by simulating  $10^4$  random network realizations that a three-node rate reduction results in 99% network feasibility.

## 1. INTRODUCTION

Optical CDMA was proposed to eliminate the electronic bottleneck imposed by the electro-optic-electro conversion at the end and intermediate nodes in optical fiber networks [1]. Optical CDMA is expected to support networks with voice, data and video applications. Each application has certain QoS requirements such as data rate, BER, probability of packet loss, packet delay, and jitter. It is very desirable to support adaptive data rates in optical CDMA networks. Recently, several approaches have been considered to provide multirate services in optical CDMA. In [2], Yashima et al. suggested optical power control and Time Hopping for multimedia applications using a single wavelength. Their approach accommodates to various data rates using only one spreading sequence by changing time-hopping rate. However, to realize such system they suggested an optical selector device which consists of a number of optical hard limiters. Optical hard limiters are not yet mature technology. Power control has been also considered in optical fast frequency hopping CDMA to provide quality of service compatibility by using variable attenuators [3]. However, the influence of network impairments, such as fiber length differences, were not considered. Disadvantages of this scheme include need for multi-wavelength transmitters and susceptibility to wavelength-dependent impairments. In [4] multi-class optical orthogonal codes were constructed while keeping the non-zero shift autocorrelation and cross-correlation properties to their minimum possible values of one. Therefore, different user transmission is highly orthogonal and near far problem can be neglected. In [5] and [6], we applied a centralized algorithm to a temporal OCDMA network in order to set the optical sources to their optimum values. It was assumed that all users applied the same bulk data rate and SIR. In this work we generalize the approach and apply concepts to a multirate system. Also, in this paper ASE is considered as the main noise source, therefore, the optical SIR before photodetection is investigated and the nonlinear behavior of the photodetection process is neglected which was considered in a separate work [7].

This paper is divided as follows: In Section 2 the multirate temporal OCDMA system based on prime codes is discussed. Optimum optical power setting using the centralized algorithm is considered in Section 3. Then in Section 4 the spectral radius of the multirate OCDMA system is investigated and used to examine the power control solution feasibility. The system spectral radius is modeled as a truncated Gaussian random variable and its upper and lower bounds are given. Moreover, a simple heuristic algorithm for

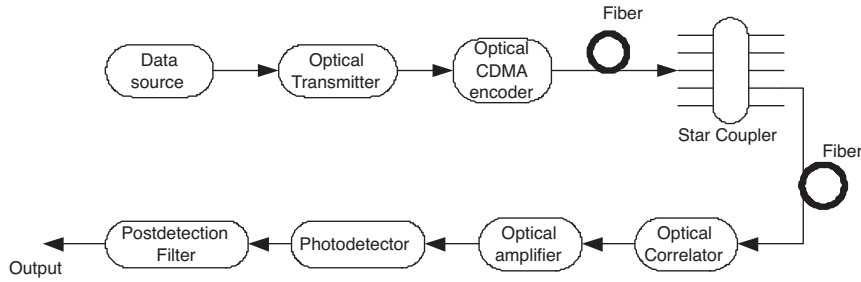


**Figure 1.** A schematic of an optical CDMA star network.

congested system relaxation is presented. Finally we give our numerical results and conclusions.

## 2. SYSTEM MODEL

The  $K \times K$  star topology considered in this paper is shown in Fig. 1. Considering the  $i$ -th user, the binary data modulates the short ( $\leq$  ratio of data bit duration to code length) optical pulse from the optical source. The transmitted optical beam power for the  $i$ -th node is denoted by  $P_i$ . Then, the optical pulse is encoded using an optical encoder that can be realized by a network of optical tapped delay lines, splitters and combiners. Incoherent optical CDMA systems are considered as positive systems, i.e., only unipolar values can be considered. Therefore, codes such as prime codes and optical orthogonal codes are specifically designed for incoherent optical CDMA applications. In order to be able to support varying code lengths and weights tunable optical encoders with adaptive optical CDMA encoding capability can be found in [8, 9]. After traversing the transmit-node fiber, star coupler and the receive-node fiber, the optical signal from all nodes is decorrelated optically by a matched decoder. Subsequently, the decorrelated signal is amplified using an optical preamplifier to compensate for the severe signal loss due to optical splitting incurred at the encoders, decoders and star coupler. Since failure of the star coupler means failure of the whole network, therefore, an active star coupler is not recommended for reliability reasons. Finally, the decoded signal is photo-detected and low-pass filtered at the optical receiver. The received and transmitted powers are related by the network attenuation matrix  $\mathbf{G}$  with  $G_{ij}$  denoting the total attenuation from  $j$ -th Tx node to  $i$ -th Rx node including fiber and splitting losses.

At the optical preamplifier output, the total received signal power is the sum of the amplified desired user correlation and unwanted users' cross-correlations. The amplified spontaneous emission (ASE) in the optical preamplifier will be the main limiting factor (in addition to the MAI) compared to thermal and shot noise at the photodetector. The ASE power at the output of the amplifier for each polarization mode is given by [10],

$$N_{sp,i} = n_{sp} h f_c (G_{amp} - 1) B_0 \quad (1)$$

where  $n_{sp}$  is the spontaneous emission factor typically around 2-5,  $G_{amp}$  is the optical amplifier gain assumed here equal to 10 dB,  $B_0$  is the optical bandwidth,  $h$  is Planck's constant, and  $f_c$  is the carrier frequency. To reduce the ASE noise power, the optical bandwidth needs to be made as small as possible. Theoretical minimum value for optical bandwidth is  $B_0 = 2R$ , where  $R$  is the bit rate, where we assume SONET OC-48 data rate.

### 3. OCDMA MULTI-RATE SUPPORT

The prime code, [11], consists of blocks each containing a single pulse. For any prime number  $q$ , a code comprises  $q$  blocks of length  $q$ . A set of code sequences of length  $N = q^2$ , derived from prime sequences of length  $q$  was derived in [12]. The procedure for code generation starts with the Galois Field,  $GF(q) = \{0, 1, \dots, j, \dots, q-1\}$ , then a prime sequence  $S_k = (s_{k0}, s_{k1}, \dots, s_{kj}, \dots, s_{k(q-1)})$  is evaluated by multiplying each element  $j$  of the  $GF(P)$  by an element  $k$  of  $GF(q)$  modulo  $q$ . Therefore,  $q$  distinct prime sequences can be obtained which are mapped into a time-mapped binary code  $c_k = (c_k(0), c_k(1), \dots, c_k(j), \dots, c_k(N-1))$  according to,

$$c_k(n) = \begin{cases} 1 & \text{for } n = s_{kj} + jq; s_{kj} = k \odot j; \\ 0 & \text{otherwise} \end{cases} \quad (2)$$

where  $j = 0, 1, \dots, q-1$  and  $\odot$  means modulo  $q$  multiplication.

To adopt the prime code for multi-rate communication, the chip duration is assumed to be fixed and the bit width is changed by a multiple integer of chips. The network supports  $M$ -QoS classes and each class has  $q_i$  codes generated according to (2). And the length of the prime signature sequence of the  $i$ -th user is related to the bit and chip durations by  $q_i^2 = T_i/T_c$ , where  $T_i$  is the data bit period of the  $i$ -th user and  $T_c$  is the chip period. Therefore, nodes with larger  $q_i$  correspond to lower data rates that map to a higher SIR

**Table 1.** Variance of cross-correlation magnitude for several primes.

$q$	<b>7</b>	<b>11</b>	<b>13</b>	<b>17</b>	<b>19</b>	<b>23</b>	<b>31</b>
<b>7</b>	0.25	0.35	0.29	0.22	0.19	0.15	0.11
<b>11</b>	0.34	0.25	0.48	0.36	0.33	0.27	0.19
<b>13</b>	0.29	0.49	0.25	0.43	0.39	0.32	0.23
<b>17</b>	0.20	0.36	0.41	0.25	0.53	0.43	0.32
<b>19</b>	0.19	0.32	0.38	0.52	0.25	0.48	0.36
<b>23</b>	0.15	0.28	0.31	0.43	0.47	0.25	0.43
<b>31</b>	0.10	0.18	0.23	0.31	0.35	0.42	0.25

in case of back-to-back equal power scenario. It is known that the prime codes can be considered as a subset of optical orthogonal codes [13, 14] and characterized by the quadruple  $(N = q_i^2, W = q_i, q_i - 1, 2)$ , i.e., prime code length of  $q_i^2$ , code weight of  $q_i$ , maximum non-zero shift autocorrelation of  $q_i - 1$ , and maximum cross-correlation of 2. The average variance of the cross-correlation magnitude between the  $i$ -th and the  $j$ -th prime signature sequences is denoted by  $\sigma_{ij}^2$  and tabulated in Table 1 for several primes, noting that  $\sigma_{ji}^2 \simeq \sigma_{ij}^2$ . It is clear also that for  $j = i \pm 1$  the value of  $\sigma_{ij}^2$  will be significant, consequently the correlation properties of the multirate code will be poor. In this work we concentrate mainly on applying power control concepts to enhance system performance, hence, we adopt the simple multirate coding scheme described above. For more advanced and complex optical prime codes with favorable correlation properties and supporting multimedia traffic see [11].

In order to get the optimum optical transmit power values we proceed by minimizing the sum of source powers under the SIR constraint,

$$\gamma_i = \frac{q_i^2 G_{amp} P_i G_{ii}}{G_{amp} \sum_{j=1; j \neq i}^K \sigma_{ij}^2 G_{ij} P_j + \sigma_{n,i}^2} \geq \gamma_{min} \quad (3)$$

where the ASE unpolarized noise power is  $\sigma_{n,i}^2 = 2N_{sp,i}$ .

Then, using matrix notations the optimum power can be evaluated using [6],

$$\mathbf{P}^* = [\mathbf{I} - \Lambda \mathbf{H}]^{-1} \mathbf{u} \quad (4)$$

where  $\mathbf{H}$  is called the interference matrix with elements,

$$H_{ij} = \begin{cases} 0 & \text{if } i = j \\ \frac{\sigma_{ij}^2 G_{ij}}{G_{ii}} & \text{if } i \neq j \end{cases} \quad (5)$$

and  $\Lambda$  is a  $K \times K$  diagonal matrix whose elements are,

$$\Lambda_i = \frac{\gamma_i}{q_i^2} \quad (6)$$

The value of  $\Lambda_i$  is set by  $\gamma_i$  and  $q_i^2$  therefore it contains information about the SIR and data rate requirements and can be considered as an indicator of the QoS level. For a single QoS class  $\Lambda$  matrix is reduced to a single element. Likewise, the elements of the scaled noise vector  $\mathbf{u}$  are given by,

$$u_i = \frac{\Lambda_i}{G_{amp} G_{ii}} \sigma_{n,i}^2 \quad (7)$$

Hence, as the required QoS is relaxed, the scaled noise power increases. It should be noted that in the above analysis the nonlinear nature of the photodetection process is neglected and only a simplified linear model is assumed.

#### 4. RATE REDUCTION ALGORITHM

In a  $K$ -node star network where each node can select its rate from a set of  $Q$  values and its target SIR from a set of  $S$  values, there are  $Q^K S^K$  possible SIR-rate combinations. For any combination, it can be shown [15] that the matrix  $[\mathbf{I} - \Lambda\mathbf{H}]$  in (4) is invertible and positive if,

$$\rho(\Lambda\mathbf{H}) < 1 \quad (8)$$

where  $\rho(\mathbf{X})$  is the spectral radius of  $\mathbf{X}$ . If  $\rho(\Lambda\mathbf{H}) \geq 1$  then the system is called infeasible which means that some or all nodes will never be able to achieve their target SIR. In this case one should relax the system QoS requirements to make it feasible by either reducing the target QoS of some nodes or one or more nodes could be switched off.

To quantify the feasibility of the power control problem solution we investigate the spectral radius in probabilistic terms. Based on extensive numerical simulations, the spectral radius could be modeled as a truncated Gaussian distribution. The mean and variance of this random variable are denoted by  $\mathbf{E}[\rho(\Lambda\mathbf{H})]$  and  $\mathbf{Var}[\rho(\Lambda\mathbf{H})]$

respectively. Therefore, the probability of feasibility can be evaluated by integrating the truncated Gaussian random variable from  $-\infty$  to 1. Hence, the probability of feasible network is,

$$\mathbf{P} [\rho(\Lambda\mathbf{H}) < 1] = 1 - Q \left( \frac{1 - \mathbf{E}[\rho(\Lambda\mathbf{H})]}{\sqrt{\mathbf{Var}[\rho(\Lambda\mathbf{H})]}} \right) \quad (9)$$

where  $Q(x)$  is the integral of the normalized Gaussian function from  $x$  to infinity. In deriving (9) we neglected a scaling factor of the truncated Gaussian (equals  $1/Q(-\mathbf{E}[\rho(\Lambda\mathbf{H})]/\sqrt{\mathbf{Var}[\rho(\Lambda\mathbf{H})]})$ ) because it is approximately unity for  $\mathbf{E}[\rho(\Lambda\mathbf{H})]/\sqrt{\mathbf{Var}[\rho(\Lambda\mathbf{H})]} > 5$ . For typical values used in this paper as will be shown in the numerical results section we have  $\mathbf{E}[\rho(\Lambda\mathbf{H})]/\sqrt{\mathbf{Var}[\rho(\Lambda\mathbf{H})]} \gg 5$ .

Since there is no closed form expression for the spectral radius  $\rho(\Lambda\mathbf{H})$  in (9) in terms of the marginal spectral radiuses of  $\mathbf{H}$  and  $\Lambda$ , therefore, we consider its upper and lower bounds as,

$$\rho(\mathbf{H}) \min(\Lambda) \leq \rho(\Lambda\mathbf{H}) \leq \rho(\mathbf{H}) \max(\Lambda) \quad (10)$$

The spectral radius of  $\mathbf{H}$  was evaluated to be equal to  $\rho(\mathbf{H}) = \sigma^2(K-1)$  [6], where we assume that the crosscorrelation variance is constant with the average value  $\sigma^2 = E\{\sigma_{ij}^2\}$ . Then, remembering (6) we can write,

$$\sigma^2(K-1) \frac{\gamma_{min}}{q_{max}^2} \leq \rho(\Lambda\mathbf{H}) \leq \sigma^2(K-1) \frac{\gamma_{max}}{q_{min}^2} \quad (11)$$

where  $\gamma_{min}, \gamma_{max}, q_{min}^2$  and  $q_{max}^2$  are the minimum target SIR, maximum target SIR, minimum code length (proportional to maximum rate), and maximum code length (proportional to minimum rate), respectively. A numerical simulation of spectral radius bounds for a 1000 realizations of a  $31 \times 31$ -network is shown in Fig. 2. Where the nodes are assumed to select random rates according to prime numbers from  $\{23, 31, 37\}$  and their target SIR from 50 to 100. It is clear that the spectral radius is bounded approximately by 0.28 and 1.42. Consequently, the designed network QoS is guaranteed if the maximum allowable SIR and the minimum code length are selected to satisfy,

$$\gamma_{max} < \frac{q_{min}^2}{\sigma^2(K-1)} \quad (12)$$

If the condition in (12) is met, then the QoS of all users will be satisfied. This will consequently leads to inefficient usage of network resources since the upper bound is far from the actual values of the spectral radius. Hence, we will consider the case when the

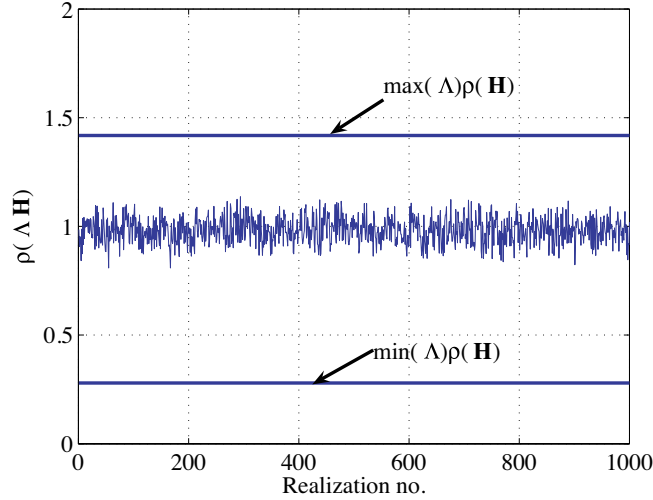


**Figure 2.** Spectral radius and its upper and lower bound for a 1000  $31 \times 31$  network realizations.

guaranteed feasibility condition is violated (8) and study the CDF of the relating spectral radius for the various QoS levels. Under certain QoS requirements the network will be in the outage condition, i.e., the spectral radius is greater than one and the target QoSs cannot be met using power control. Therefore, we apply a removal algorithm to improve system feasibility. The optimal load control or removal algorithms is generally an NP-problem and a closed form solution has not been found. Therefore, several heuristic removal algorithms have been investigated [16]. Instead of switching off some nodes completely as in [16] we propose a modified removal algorithm to keep all the nodes on but with reduced data rate. We call this algorithm as the rate reduction (RR) algorithm. We categorize the RR algorithm according to the number of nodes  $k$  subject to reducing their rate as  $k$ -RR. Therefore, 1-RR means that only one node is subject to rate reduction, 2-RR refers to rate reduction in two nodes, and so on. We use an indicator variable to select the candidate nodes subject to  $k$ -RR as,

$$I_i = \frac{\Lambda_i}{L_i^{tx}} \quad (13)$$

Therefore, the indicator variable is maximum for nodes with the highest QoS requirement and shortest fibers from the star coupler, since these nodes are expected to cause the highest interference in

the network. If the rate of the nodes with the highest indicators are reduced, then the upper bound in (11) decreases. Consequently, the mean and variance of the truncated Gaussian spectral radius will be decreased leading to increased probability of feasibility according to (9). Hence, the  $k$ -RR algorithm is summarized as follows.

- (i) Arrange the nodes in descending order following (13).
- (ii) Reduce the rate of the first node on the list by one step.
- (iii) Check the feasibility using (8), if the system is feasible then stop.
- (iv) Reduce the rate of the second node on the list by one step, if the system is feasible then stop.
- (v) Repeat the same until the  $k$ -th node.
- (vi) If the system is still infeasible then start over at step (2).

We assume here that all nodes have the same priority and if a node reaches its minimum rate then it is not included in the RR procedure. Other variations of the above procedure are possible. For example, it can be implemented such that after the rate of the highest indicator is reduced the system feasibility is checked and if infeasible then recalculate the indicators again and reduce the highest one and so on.

## 5. NUMERICAL RESULTS

First we consider the sensitivity of the power control solution to the network spectral radius by plotting the average distance between the target SIR  $\bar{\gamma}_i$  and actual SIR  $\gamma_i$  as,

$$e_\gamma = \frac{1}{K} \sum_{i=1}^K \left( \frac{\bar{\gamma}_i - \gamma_i}{\bar{\gamma}_i} \right)^2 \times 100\% \quad (14)$$

For a  $31 \times 31$  star network using a single rate with prime number of  $q = 31$  the mean SIR error is shown in Fig. 3. At  $\rho(\Lambda\mathbf{H}) = 1.5$  and 2, the SIR error is approximately 40% and 95% respectively. This indicates that the power control solution is highly sensitive to a spectral radius greater than 1 in terms of the SIR error. Therefore, it is important to keep the spectral radius as close as possible but less than one.

Next we consider a star coupled  $31 \times 31$  system where the nodes can join one of three rates with  $q = \{23, 31, 37\}$ . The fiber lengths are selected such that the nodes are randomly distributed over an area centered at the star with a radius from 2.5 to 50 Km. The applied system parameters are listed in Table 2. The 24-th node has the highest

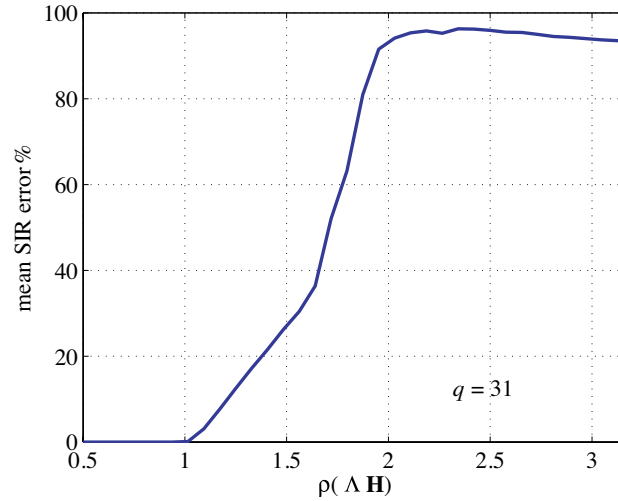


**Figure 3.** Mean SIR error vs spectral radius.

SIR and the first node has the smallest SIR (sixth column) if all nodes transmit with the maximum allowable optical power (10 dBm). The last column in the table shows the normalized optimum power vector. Since  $\rho(\Lambda \mathbf{H}) = 1.01$ , the system is marginally infeasible and the SIR values after applying optimized power levels (last column in Table 2) are slightly less than the target SIR and the SIR error is less than 1% as deduced from Fig. 3.

In Fig. 4, the target SIR of one node is changed from 17 to 23 dB while fixing all other nodes to 18.7 dB. It shows that the spectral radius is clustered in groups of equal code weight. Because of higher processing gain, the low rate nodes (labeled “c”) have the smallest impact on the spectral radius. The target SIR of the high rate nodes (labeled “a”) have the highest impact on the network feasibility. Fig. 5 shows that the spectral radius is decreased below one more rapidly by reducing the rate of high rate nodes as compared to low rate nodes. This is in agreement with the indicator selection adopted in (13).

Finally, we generate  $10^4$  network realizations from which we calculate the CDF of the spectral radius for the Rate Reduction Algorithm of section IV (6). For the applied network parameters, the mean and variance of the network spectral radius are found to be 0.98 and .0036 respectively. Using (9) then it is found that, when no RR is applied, around 62% of the time QoS network requirements can be fulfilled. The same can be deduced from Fig. 6 which indicates the validity of the truncated Gaussian assumption. The network feasibility

**Table 2.**  $31 \times 31$  star network. Fiber lengths ( $L_i^{tx}$ ,  $L_i^{rx}$ ), user code prime number  $q_i$ , target SIR  $\bar{\gamma}_i$ , SIR without power control  $\hat{\gamma}_i$ , SIR with power control  $\gamma_i$ , and normalized optimum power  $P_i^*$ .

$i$	$L_i^{tx}$ [Km]	$L_i^{rx}$ [Km]	$q_i$	$\bar{\gamma}_i$	$\hat{\gamma}_i$	$\gamma_i$	$P_i^*$ [dB]
1	47.65	37.85	37	90	34.12	86.26	0
2	13.1	23.35	23	70	81.56	69.32	-4.42
3	31.15	46.75	31	100	49.47	95.81	-1.1
4	25.35	24.35	31	75	64.88	73.87	-3.42
5	44.8	22.1	37	70	38.89	68.58	-1.59
6	38.6	42.65	37	95	51.86	90.1	-1.6
7	23.9	27.2	31	75	69.45	73.71	-3.72
8	2.85	11.7	23	60	134.3	59.66	-7.13
9	41.45	34.25	37	85	45.36	82	-1.46
10	23.35	42.25	31	95	71.15	91.75	-2.86
11	31.55	2.9	31	50	48.49	49.72	-3.89
12	40.05	34.7	37	85	48.38	81.94	-1.74
13	46.25	20.2	37	70	36.28	68.7	-1.29
14	37.45	41.95	37	95	54.6	90.26	-1.82
15	10.45	26.15	23	75	93.13	74.17	-4.7
16	21.45	36.05	31	85	77.72	82.81	-3.69
17	46.9	22.6	37	70	35.16	68.55	-1.16
18	46.05	16.6	37	65	36.58	63.98	-1.64
19	21.7	11.1	31	60	76.83	59.51	-5.09
20	44.9	11.25	37	60	38.57	59.26	-2.2
21	4.75	34.75	23	85	123	83.59	-5.34
22	18.95	16.5	31	65	87.31	64.32	-5.3
23	41.05	28	37	75	46.04	73.02	-2.04
24	2.45	9.2	23	55	137.9	54.72	-7.61
25	8.65	35.5	23	85	102	83.54	-4.56
26	11.7	20.15	23	70	88.05	69.41	-4.75
27	11.5	43.3	23	95	88.9	92.66	-3.55
28	31	43	31	95	49.39	91.66	-1.31
29	15.05	30.5	23	80	75.06	78.91	-3.53
30	11.55	25.85	23	75	88.74	74.18	-4.5
31	2.7	45.2	23	95	136.3	92.45	-5.32

is increased to around 87%, 97%, and 99% using the 1-RR, 2-RR and 3-RR, respectively. Hence, by using a 3-RR algorithm one can find a feasible network for 99% of the time.

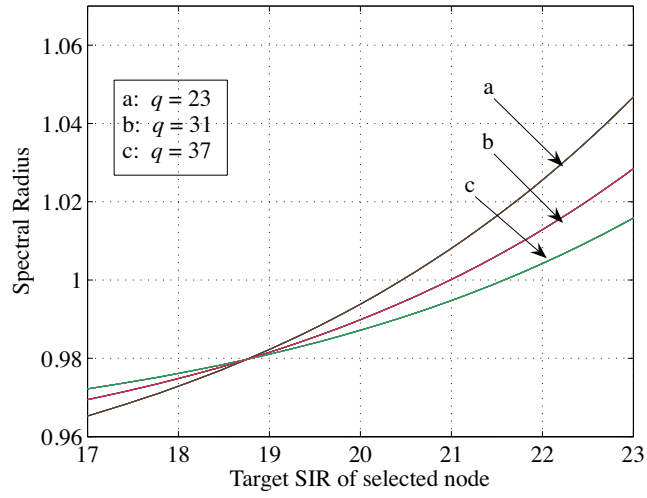


Figure 4. Target SIR effect on spectral radius.

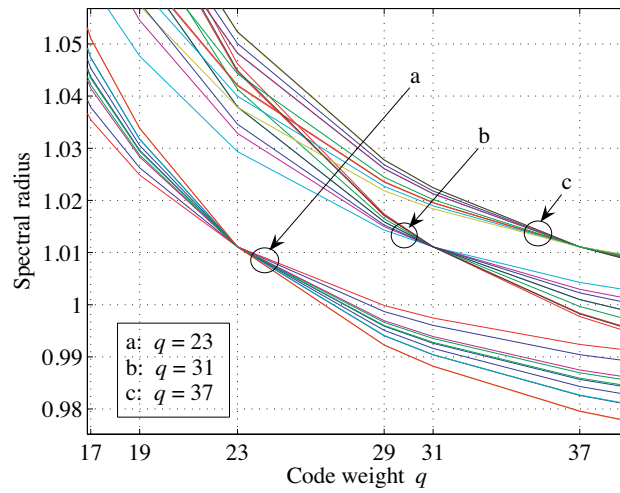
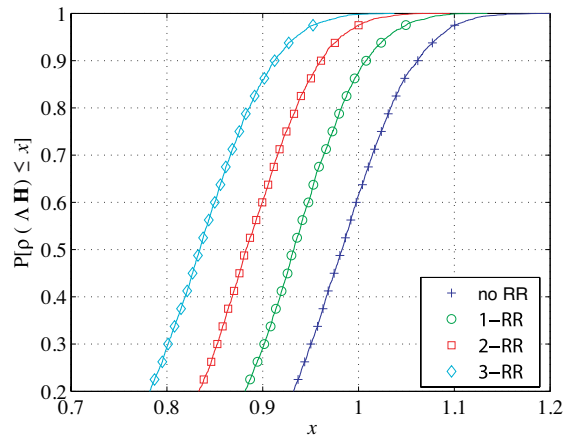


Figure 5. Code weight effect on spectral radius.



**Figure 6.** CDF of spectral radius with different RRs.

## 6. CONCLUSIONS

We applied centralized power control to evaluate the optimum optical power for a multirate optical CDMA network. A network with multiple length temporal prime encoding was considered. We noticed that nodes with longer fibers and higher QoS will use the highest power. Based on large number of network realizations, the spectral radius of the system was modeled as a truncated Gaussian random variable and then the feasibility of the solution was written in terms of the model parameters. In this paper we proposed novel Rate Reduction Algorithm in order to increase feasibility of network's power control. Efficiency of our approach was then inspected by Monte Carlo -type simulations.

## REFERENCES

1. Kitayama, K., H. Sotobayashi, and N. Wada, "Optical Code Division Multiplexing (OCDM) and its application to photonic networks," *IEICE Trans: Fundamentals*, Vol. E82-A, No. 12, 2616, Dec. 1999.
2. Yashima, H. and T. Kobayashi, "Optical CDMA with time-hopping and power control for multimedia networks," *Journal of Lightwave Tech.*, Vol. 21, No. 3, 695–702, March 2003.
3. Intay, E., H. Shalaby, P. Fortier, and L. Rusch, "Multirate optical fast frequency-hopping CDMA system using power control," *Journal of Lightwave Tech.*, Vol. 20, No. 2, 166–177, February 2002.

4. Tarhuni, N., T. Korhonen, E. Mutafungwa, and M. Elmusrati, "Multi-class optical orthogonal codes for multi-service optical CDMA networks," *Journal of Lightwave Tech.*, Vol. 24, No. 2, February 2006.
5. Tarhuni, N., M. Elmusrati, T. Korhonen, and E. Mutafungwa, "Multi-access-interference mitigation using power control in optical-CDMA star networks," *IEEE International Conference on Comm. ICC 2005*, 1593–1597, May 16–20, 2005.
6. Tarhuni, N., T. Korhonen, M. Elmusrati, and E. Mutafungwa, "Power control of optical CDMA star networks," *Elsevier Optic Comm. Journal*, in press.
7. Tarhuni, N., M. Elmusrati, and T. Korhonen, "Nonlinear power control for asynchronous fiber-optic CDMA networks," *IEEE International Conference on Comm. ICC 2006*, accepted, will be held on June 11–15, 2006, Istanbul, Turkey.
8. Baby, V., B. C. Wang, L. Xu, I. Glesk, and P. R. Prucnal, "Highly scalable serial-parallel optical delay line," *Optics Communications*, Vol. 218, 235–242, 2003.
9. Zhang, J. and G. Picchi, "Tunable prime code encoder/decoder for all-optical CDMA application," *Elect. Letters*, Vol. 29, 1211–1212, 1993.
10. Ramaswami, R. and K. N. Sivarajan, *Optical Networks, a Practical Perspective*, Morgan Kaufmann Publishers, 1998.
11. Yang, G. C. and W. C. Kwong, *Prime Codes with Applications to CDMA Wireless and Optical Networks*, Artech House, 2002.
12. Prucnal, P., M. Santoro, and T. Fan, "Spread spectrum fiber-optic local area network using optical processing," *Journal of Lightwave Technology*, Vol. 4, No. 5, 547–554, 1986.
13. Salehi, J., "Code division multiple access techniques in optical fiber networks—Part I: Fundamental concepts," *IEEE Trans. Comm.*, Vol. 37, 824, August 1989.
14. Chung, F. R. K., J. A. Salehi, and V. K. Wei, "Optical orthogonal codes: Design, analysis, and applications," *IEEE Trans. on Info. Theory*, Vol. 35, No. 3, May 1989.
15. Gantmacher, F., *The Theory of Matrices*, Chelsea Publishing Company, 1964.
16. Elmusrati, M., N. Tarhuni, R. Jntti, and H. Koivo, "Distributed minimum outage removal algorithm for multi-rate CDMA wireless communication systems," *Proc. of the 6th Nordic Signal Processing Symp. NORSIG*, 256–259, ESPOO, Finland, June 9–11, 2004.